



iSBatch: a batch-processing platform for data analysis and exploration of live-cell single-molecule microscopy images and other hierarchical datasets

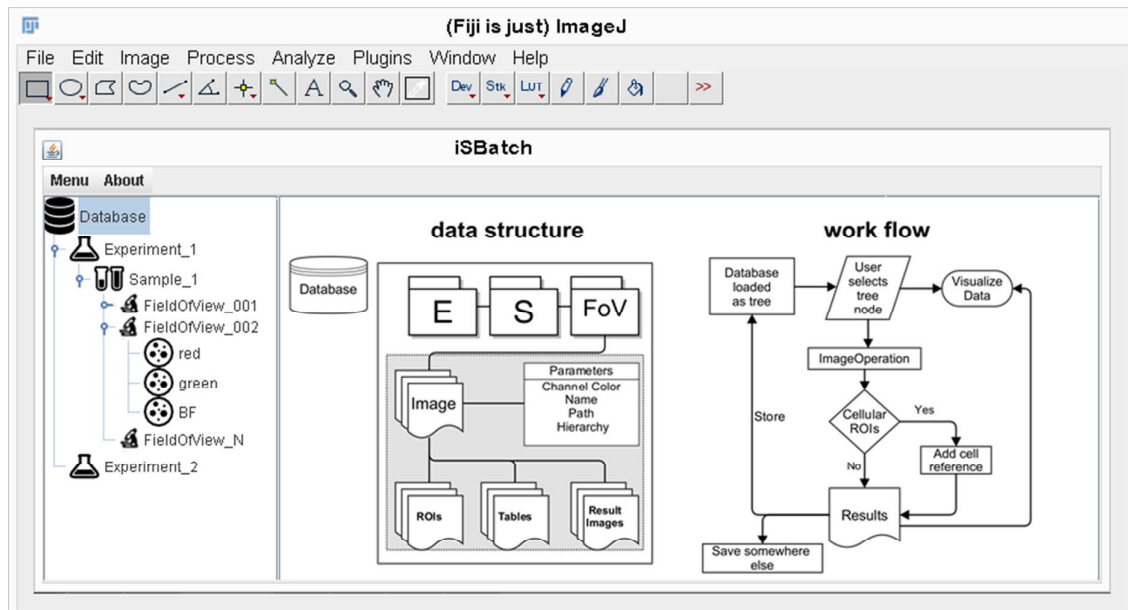
Journal:	<i>Molecular BioSystems</i>
Manuscript ID:	MB-MET-05-2015-000321.R1
Article Type:	Method
Date Submitted by the Author:	10-Jul-2015
Complete List of Authors:	Armini Caldas, Victor Emanoel; University of Groningen , Zernike Institute for Advanced Materials Punter, Christiaan; University of Groningen, Zernike Institute for Advanced Materials Ghodke, Harshad; University of Groningen, Zernike Institute for Advanced Materials Robinson, Andrew; University of Groningen, Zernike Institute for Advanced Materials van Oijen, Antoine; University of Groningen, Zernike Institute for Advanced Materials

Table of contents accompanying

iSBatch: a batch-processing platform for data analysis and exploration of live-cell single-molecule microscopy images and other hierarchical datasets

Victor E. A. Caldas, Christiaan M. Punter, Harshad Ghodke, Andrew Robinson and Antoine M. van Oijen

iSBatch: an ImageJ plugin for fast evaluation of analysis pipelines and visual exploration of datasets.



1 **iSBatch: a batch-processing platform for data analysis and exploration of live-cell single-**
2 **molecule microscopy images and other hierarchical datasets**

3 Victor E. A. Caldas¹, Christiaan M. Punter¹, Harshad Ghodke¹, Andrew Robinson¹ and
4 Antoine M. van Oijen^{1*}

5

6

7 ¹Zernike Institute for Advanced Materials, Centre for Synthetic Biology, University
8 of Groningen, The Netherlands

9 *Corresponding author. Current address: School of Chemistry, University of Wollongong,
10 Wollongong NSW 2522, Australia.

11 Phone: +61-(2)4221 4780. Fax: +61-(2)4221 4287. Email: vanoijen@uow.edu.au

12

13 Running title: Batch processing tool for single-molecule single-cell images

14

15

16 **Key words:** single-molecule microscopy, live-cell imaging, fluorescence, batch processing

17

18 Abstract

19 Recent technical advances have made it possible to visualize single molecules inside live cells.
20 Microscopes with single-molecule sensitivity enable the imaging of low-abundance proteins,
21 allowing for a quantitative characterization of molecular properties. Such data sets contain
22 information on a wide spectrum of important molecular properties, with different aspects
23 highlighted in different imaging strategies. The time-lapsed acquisition of images provides
24 information on protein dynamics over long time scales, giving insight into expression dynamics
25 and localization properties. Rapid burst imaging reveals properties of individual molecules in real-
26 time, informing on their diffusion characteristics, binding dynamics and stoichiometries within
27 complexes. This richness of information, however, adds significant complexity to analysis
28 protocols. In general, large datasets of images must be collected and processed in order to
29 produce statistically robust results and identify rare events. More importantly, as live-cell single-
30 molecule measurements remain on the cutting edge of imaging, few protocols for analysis have
31 been established and thus analysis strategies often need to be explored for each individual
32 scenario. Existing analysis packages are geared towards either single-cell imaging data or *in vitro*
33 single-molecule data and typically operate with highly specific algorithms developed for particular
34 situations. Our tool, iSBatch, instead allows users to exploit the inherent flexibility of the popular
35 open-source package ImageJ, providing a hierarchical framework in which existing plugins or
36 custom macros may be executed over entire datasets or portions thereof. This strategy affords
37 users freedom to explore new analysis protocols within large imaging datasets, while maintaining
38 hierarchical relationships between experiments, samples, fields of view, cells, and individual
39 molecules.

40

41

42

43

44

45 Introduction

46

47 Fluorescence microscopy has played an enormously important role in our understanding of biology.

48 By tagging molecules of interest with fluorescent proteins, the dynamics of many cellular systems

49 have been observed within live cells. However, many important cellular processes are carried out by

50 proteins that are expressed at very low levels and are therefore undetectable using standard

51 fluorescence microscopes^{1,2}. Proteins that replicate and repair chromosomes in bacteria, for

52 example, are often expressed at a level of less than 100 molecules per cell³. The recent development

53 of fluorescence microscopes with single-molecule sensitivity is allowing us to peer into this world for

54 the first time.

55 In addition to extending the sensitivity of established wide-field microscopy techniques, single-

56 molecule microscopes allow rapid image sequences to be recorded that reveal the movements of

57 individual molecules. Single-molecule microscopes can be used to record wide-field video-rate

58 movies, with exposure times of 10–100 ms for individual images. On this timescale, fluorescent

59 signals from molecules that diffuse freely within the cytosol of a bacterial cell or within the

60 organelles of eukaryotic cells, blur out over the accessible volume in the cell or organelle due to

61 rapid diffusion rates ($D \sim 1\text{--}10 \mu\text{m}^2/\text{s}$ ⁴⁻⁶). On the other hand, molecules that bind relatively static

62 structures, such as chromosomal DNA, exhibit a much smaller diffusion constant and thus present as

63 static foci of diffraction-limited size ($\sim 300 \text{ nm}$). Similarly, molecules that diffuse slowly, such as

64 proteins associated with cell membranes, present discrete foci that move along the cell periphery.

65 Movements of such single-molecule foci can be tracked in order to observe events that lead to a

66 change in diffusion rate, for example, binding of molecules to DNA or other large structures. At the

67 same time, intensities of foci in conjunction with photobleaching can be tracked in order to measure

68 the number of fluorescent molecules giving rise to each focus, allowing the compositions of

69 molecular complexes to be determined⁷.

70

71 These extra layers of information provide fresh insight into the behaviors of molecules within cells,
72 but also pose a problem for the scientists who study them: in order to obtain sufficient statistics to
73 generalize observations, data must be recorded for many molecules, within many cells. Single-
74 molecule imaging requires the use of high-magnification, high-numerical aperture objectives⁶,
75 limiting the size of the field-of-view and thus the number of cells that can be observed
76 simultaneously. Typically, to discern statistically significant outcomes, hundreds of images must be
77 recorded for a particular a live-cell single-molecule sample. That sample may contain hundreds of
78 fields, potentially containing hundreds of time-points, up to thousands of cells of which each contain
79 a handful of foci. Furthermore, it is often desirable to collect images in two or more fluorescence
80 colors in order to correlate the behaviors of multiple types of molecules, as well as bright-field or
81 phase-contrast images to define cell boundaries. These data are highly hierarchical in nature and
82 efficient analysis is only possible when the hierarchical relationships between the different levels in
83 the data are maintained during analysis.

84 A software package for single-molecule analysis in live-cells should meet four basic conditions.
85 Firstly, it should allow for hierarchical classification of images and regions-of-interest (ROIs): samples
86 contain fields of view (images), fields of view contain ROIs that capture individual cells (cell ROIs),
87 and cells contain ROIs that define single-molecule foci (focus ROIs). Secondly, it should allow for
88 analysis over both long and short time scales, resulting in the generation of different data structures:
89 in time-lapse datasets there is one cell ROI per time point, whereas in rapid-imaging mode each cell
90 ROI is typically used to analyze fluorescence signals over many time-points (**Fig. 1**). Thirdly, and most
91 importantly, a package for live-cell single-molecule analysis should be highly flexible and allow for
92 exploration of new analysis techniques. Finally, the source code used in the package be made
93 available to users so that researchers can fully understand the algorithms they use⁸.

94 Sophisticated packages for both cell analysis and single-molecule analysis are currently available,
95 however none meet all of the requirements listed above⁹. Commercial packages typically offer out-

96 of-the-box solutions to a particular set of problems, often involve high licensing fees and utilize
97 undisclosed source code, limiting the users' ability to adapt the software or to add their own
98 customized code. CellProfiler¹⁰ (and its extension CellProfiler Analyst¹¹) is a free open-source package
99 with a robust set of algorithms for analysis of 2D images. CellProfiler excels at automated assignment
100 of cellular phenotypes, as well as identification of sub-cellular particles. However, with its focus on
101 high-throughput screening data, the package provides little support for time-resolved studies.
102 MicrobeTracker¹² allows users to conveniently assign outlines for microbial cells within time-lapse
103 datasets and provides some support for characterization of foci. It is, however, not suitable for
104 analysis of rapid-imaging data and is not geared towards exploration of new analysis methods. In
105 addition, while MicrobeTracker itself is free, it runs within an environment that requires a paid
106 licence (Matlab). Single-molecule packages such as the Mosaic Suite¹³, as well as plugin collections,
107 such as GDSC ImageJ Plugins¹⁴ offer a myriad of analysis methods for single-molecule image
108 processing, but are intended for *in vitro* analysis and thus lack the hierarchical classification systems
109 that are required for the analysis of data derived from cellular systems. A significant advantage of
110 these packages, however, is that they are extensions of the popular image-analysis platform
111 ImageJ^{15,16}, which is extremely flexible, supported by a strong user community and a wealth of user-
112 written extensions. Unfortunately, ImageJ is geared towards working with individual files, making
113 hierarchical analysis strategies difficult to implement.

114 Flexible software that links analysis routines used in single-molecule imaging with those used in live-
115 cell imaging is required for researchers to keep up with the rapid development of new imaging
116 techniques. Ideally, one would be able to utilize ImageJ to develop code for new analysis routines,
117 whilst being able to easily accommodate data structures that are large, hierarchical and multi-
118 dimensional.

119 We present a free open-source ImageJ plugin, iSBatch, which allows users to use batch processing to
120 treat files within hierarchical datasets in a straightforward manner. Routines built into ImageJ¹⁵,

121 downloadable plugins and even user-written macros can be executed across any level of the dataset
122 hierarchy. This strategy dramatically simplifies the often cumbersome tasks of scripting and data
123 management, allowing users to run scripts over their entire datasets or portions thereof. Our tool
124 complements existing single-cell and single-molecule analysis packages by allowing cell and focus
125 ROIs generated in single-cell packages to be applied across hierarchical time-lapse and rapid-imaging
126 datasets, with complete flexibility in choice of analysis methods.

127 **Results and Discussion**

128 iSBatch is straightforward to use, platform independent, and requires only ImageJ and Java Virtual
129 Machine, which are freely available. iSBatch provides an interface to explore data in hierarchical
130 datasets. Its graphical user interface (GUI) provides an intuitive means for controlling the operations
131 and manipulating datasets of any size. iSBatch incorporates a powerful adapter for the ImageJ macro
132 interpreter, allowing users to implement existing or newly written macros within the data hierarchy.
133 Data is stored in an SQL database and displayed in a tree format for manipulation (**Fig. 2a**). The
134 database format assists in managing the transfer and back-up of large imaging datasets, which may
135 contain hundreds or even thousands of images and can be prone to errors when handled manually
136 ¹⁷. A file named 'iSBatch.zip', which contains the plugin, its source code and user manual, is included
137 in the online Supplementary Material. To help to illustrate the concepts in the following sections of
138 this report, we also include an example dataset containing three Experiments in the Supplementary
139 Material.

140 **Data Structure and Graphical User Interface (GUI)**

141 The fundamental unit of iSBatch is the image itself. Each image belongs to a Field of View,
142 representing the region of the sample that was imaged by the microscope. A collection of Fields of
143 View is called a Sample, and a collection of Samples is called an Experiment. This hierarchy is
144 assigned to each image by placing hierarchy parameters alongside the image within an image object.
145 Image objects may contain an unlimited number of additional parameters. Within iSBatch, image

146 objects contain information on the nature of the image, for example identifiers for color channels,
147 metadata generated during operations, such as peak tables and image projections, as well as ROIs
148 that designate the positions of cells and foci. A dedicated dialog guides the import of imaging data
149 and assures compatibility with iSBatch. There is no specific requirement for file name structure,
150 however we suggest the inclusion of a useful identifier for the imaging channel (e.g. 514.tif, BF.tif,
151 GFP.tif).

152 The general workflow within iSBatch is straightforward (**Fig. 2b**). In short, the user selects which
153 subset needs to be processed, chooses the operation to be performed and indicates either to save
154 results and images to disc or keep it in the database. The graphic user interface is divided into
155 subpanels containing the navigation tree, file lists, buttons to run built-in functions or custom
156 macros and a log panel (**Fig. 2c**). The GUI also has buttons to add images to the data structure, as
157 well as cell ROIs generated in ImageJ or in MicrobeTracker¹⁸.

158 We have included several operations commonly used in single-molecule analysis within iSBatch, such
159 as functions to correct images for uneven illumination, find and fit peaks inside or outside of cells,
160 and basic peak table operations. These operations will be explored in detail in the form of case
161 studies in the sections below.

162 **Case studies**

163 To demonstrate the applicability of our iSBatch software we present here a case in which the *custom*
164 *macro interpreter* was applied to a dataset, as well as two detailed case studies based on the most
165 common types of data generated by single-molecule single-cell measurements: rapid-acquisition
166 movies and time-lapse series. We imaged *Escherichia coli* cells in which two different subunits of the
167 replisome were tagged with fluorescent proteins at their carboxy-termini; the ϵ subunit (DnaQ gene)
168 is tagged with red mKate2 (DnaQ-mKate2) and the τ subunit (DnaX gene) is tagged with yellow YPet
169 (DnaX-YPet). The *E. coli* replisomes contain ten different proteins, each at different copy numbers,
170 including up to three molecules of τ (a component of the clamp loader complex) and three

171 molecules of ϵ (proof-reading exonuclease)³. Replisome proteins are of particular interest for single-
172 molecule studies^{3,19} both because of their biological role of importance (replisomes duplicate the
173 genome prior to cell division)²⁰ and because the replisomal proteins are present at extremely low
174 levels within cells. A single *E. coli* cell produces only about 100 molecules of τ per cell and ~250
175 molecules of ϵ^3 .

176 The example data is comprised of a single database containing three experiments, labeled RA_DnaX-
177 YPet, RA_DnaQ-mKate2 and TimeLapse). RA_DnaX-YPet and RA_DnaQ-mKate2 are Rapid Acquisition
178 (RA) experiments (500 times 34 ms) that each contain three samples recorded at different excitation
179 laser powers. Each of these samples contains 10 fields of view. TimeLapse contains just one sample
180 and 10 fields of view (50 ms every 20 min, repeated for 400 minutes). RA_DnaX-YPet includes 134
181 cell selections, RA_DnaQ-mKate2 contains 107 and TimeLapse contains 10 fully tracked cells. iSBatch
182 assumes that, if no cell ROIs are provided, the entire image is selected. This scenario is applicable to
183 analyses that do not rely on cell outlines, such as reconstruction of super-resolution images by PALM
184 ^{21,22} or STORM ²³, or even to the analysis of *in vitro* single-molecule data.

185 When loaded into iSBatch, our datasets appear in the operation panel (**Fig 2c**). Selecting a node
186 within one of the datasets allows image-processing operations to be executed across all images
187 falling under that node. For example, when the user selects the node RA_DnaQ in the tree and the
188 operation *flatten*, iSBatch guides the user through the steps required for image flattening and
189 correction for the unevenness of the beam profile (more details found in the User Manual –
190 Supplementary Materials) within selected images in the RA_DnaQ experiment. Next, iSBatch
191 assumes that operations will be performed on the resulting flattened images as will be shown in the
192 following sections.

193 **Custom macro interpreter**

194 The ImageJ support to macros is a powerful tool to execute a sequence of operations in an image.
195 Traditionally, in order to apply basic ImageJ functions across portions of a dataset, the user has to

196 write sequences of steps and functions to navigate through the folders, to identify the required files,
197 and to save the results. Even small changes in the folder or file structure prevent the code from
198 running properly and troubleshooting becomes a daunting task. iSBatch, via its *custom macro*
199 *interpreter*, provides the necessary tools to automatize these steps (**Fig. 3**).

200 Within our rapid acquisition data, for instance, stacks exported from the microscope contain dark
201 frames at the beginning of the image series, resulting from a small delay before the opening of the
202 laser shutter. The *custom macro interpreter* can be easily used to trim stacks in order to remove
203 these frames. There are two possibilities of implementation: an experienced user may just write a
204 macro to trim one image and then use it within the *custom macro interpreter*; or could take
205 advantage of ImageJ *Macro Recorder* – a panel that stores all commands performed by the user
206 while processing an image– and then simply paste the sequence of steps into the iSBatch *custom*
207 *macro interpreter*. The user then can analyse the images further in a statistical package, like R^{24} .

208 **Rapid-Acquisition Analysis**

209 Rapid-Acquisition experiments usually result in a stack of fluorescence images, containing hundreds
210 or thousands of individual frames, acquired at rapid frame rates (typically continuous series of
211 frames, 10-100 ms duration each, with a total duration of seconds), as well as a bright-field image
212 enabling the identification of cell boundaries in cases of low fluorescence signals. This type of
213 imaging allows the behaviors of individual molecules to be monitored in real time. It is typically used
214 to count molecules within foci, to count the total number of molecules in cells, to measure diffusive
215 behavior and to observe binding kinetics^{1,3,7}.

216 In our datasets, DnaX-YPet and DnaQ-mKate2 frequently are associated with DNA-bound replisomes,
217 and as a result form immobile foci on the imaging timescale (34 ms). We used iSBatch to detect foci
218 and measure their integrated intensities using the *peak fitter* operation in a selected node (**Fig. 4a**).
219 The built-in *peak fitter* fits each peak to a Gaussian profile using least-squares fitting. It takes into
220 account sources of noise, such as general background noise, and uses a non-symmetric 2D Gaussian,

221 so peaks can be later filtered based on their symmetry²⁵. The properties of foci in single-molecule
222 single-cell measurements can vary between experiments, depending on the brightness of the
223 fluorophore and the amount of background fluorescence arising from cellular auto fluorescence. It is
224 therefore desirable to be able to explore parameters such as peak-detection thresholds for
225 individual samples. iSBatch automatically stores peak tables generated from the *peak fitter* module,
226 appending the results with the values of key parameters used. In this way, the user can explore
227 different parameters and plot the resulting peaks lists in an external plotting or statistical analysis
228 package, for example *GNU Octave*²⁶ or *R*²⁴. In our example data, we see that for both fluorescent
229 species the intensities of peaks increase with higher excitation power, as expected (**Fig. 4b**).

230 Foci containing fewer than about 10 molecules show step-wise photobleaching behavior that can be
231 used to quantify the number of fluorescent molecules within each focus^{5,27}. Using iSBatch,
232 trajectories of intensity *versus* time can be generated for foci using the *traces* module. This can be
233 done in two different ways. One option is to produce an average projection of each image stack,
234 assign focus ROIs in the projected image using *peak finder* and measure the integrated intensity
235 under each ROI for each frame of the stack. The second option is to use *peak fitter* to measure foci
236 throughout the entire stack of a 'Field of View' and then use *track* to identify foci falling within a
237 small, user-defined search radius of a focus that appeared in the first frame and produce a time-
238 ordered list of their intensities. As expected, traces for DnaQ-mKate2 show step-wise
239 photobleaching behavior (**Fig. 5**). Intensity levels within traces can be automatically assigned using
240 the *change-point analysis* (**Fig. 5c, red lines**). This algorithm estimates the time point at which the
241 statistical properties of a sequence change, e.g. photobleaching causing a discrete jump in intensity
242 followed by a period of constant intensity^{28,29}.

243 As well as quantifying the number of molecules in each focus, the single-molecule intensity
244 determined within the *change-point* module can be used to determine the total number of
245 molecules in each cell. For this, it is necessary to have ROIs defining the cell boundaries. These can

246 be generated in ImageJ or imported from MicrobeTracker using the module *MicrobeTracker I/O*. In
247 iSBatch, the total fluorescence signal originating from a cell as it photobleaches can be measured by
248 applying the *cell intensity* operation to a batch (**Fig. 6**). Comparing the three DnaQ-mKate2 samples
249 within the RA_DnaQ experiment (**Fig. 6a**), we observe that DnaQ-mKate2 photobleaches faster at
250 higher laser excitation intensities, as expected (**Fig. 6b**). Comparing the OD1 samples between the
251 RA_DnaX and RA_DnaQ experiments (**Fig. 6c**), we observed that YPet photobleaches faster than
252 mKate2 (**Fig. 6d**), as expected^{30,31}. Using the *cellular concentration* operation, the amplitudes of
253 these decays (representing the total fluorescence of the cell) is divided by the intensity of a single
254 molecule in order to obtain the number of molecules in that cell and the cellular concentration. For
255 DnaX-YPet and DnaQ-mKate2 we measure 110 ± 35 and 95 ± 22 molecules per cell respectively.
256 Based on the mean volume of cells as measured from bright field images (4.6 ± 0.9 fL), these values
257 correspond to concentrations of approximately 23 and 20 nM for DnaX-YPet and DnaQ-mKate2
258 respectively.

259 Rapid-acquisition imaging can also be used to measure the movements of molecules. Single-particle
260 tracking can be used to measure the diffusional motions of molecules. In iSBatch this operation is
261 implemented in the *tracking* module. Here foci within the tables generated by *peak fitter* are
262 assigned to trajectories if they fall within a set distance on consecutive frames and, optionally, are
263 within the same cell ROI (**Fig. 7a**). These trajectories can be used to build step-size distributions or
264 mean-square displacement plots that allow for measurement of properties such as diffusion
265 coefficients. For DnaQ-mKate2, which present long-lived trackable foci, we observe two populations:
266 one with low diffusion coefficients corresponding to molecules bound to DNA, and one with higher
267 diffusion coefficients corresponding to freely-diffusing molecules⁵ (**Fig. 7b**).

268 Time-Lapse Analysis

269 Time-lapse datasets consist of image stacks containing equal numbers of bright-field images and
270 fluorescence images, with individual frames corresponding to measurements at periodically sampled

271 time-points. Time-lapse measurements can be used to monitor temporal changes in the expression
272 level of a protein, the number of foci within cells, or the localization of proteins within cells. With the
273 availability of automated microscopes, we can monitor hundreds cells in several fields of view over a
274 period of minutes to days³².

275 Our example dataset, TimeLapse, contains images of cells expressing DnaX-YPet and DnaQ-mKate2
276 recorded over 400 minutes. Using the module *cell intensity*, we measured the levels of each
277 fluorescent protein for ten cells over time. The levels of DnaX and DnaQ remain relatively constant
278 throughout the measurement (**Fig. 8a**). Using the number of foci detected by *peak finder* or *peak*
279 *fitter*, we quantified the number of DnaX-YPet and DnaQ-mKate2 foci observed over time. As
280 expected, cells periodically changed between zero, one, two and occasionally three foci (**Fig. 8b**).
281 Because we imaged in time-lapse mode, movie sequences of individual cells could be synchronized
282 to the beginning of the cell cycle. This analysis shows that after division, daughter cells contain one
283 foci on average, then the increases to two foci later in the cell cycle (**Fig. 8c**). If cell ROIs have been
284 imported from MicrobeTracker, it is possible to produce maps of focus locations within cells using
285 the *location maps* module. MicrobeTracker ROIs consist of high-resolution meshes, allowing the
286 relative positions of foci to be mapped to their relative cellular coordinates. For DnaX-YPet and
287 DnaQ-mKate2 cells, one focus was present from 0 to 40 min after birth (**Fig. 8c**). This focus was
288 located close to the mid-cell position (**Fig. 8d**). In contrast, 60 to 120 min after division, cells
289 exhibited two foci (**Fig 8c**). These foci were more evenly distributed through the entire cell (**Figure**
290 **8d**).

291 **Materials and Methods**

292 **Implementation**

293 **Software**

294 iSBatch is a Java 1.6-based plugin for ImageJ¹⁵ (version 1.49d) or its distribution Fiji³³. iSBatch is
295 designed for quick evaluation of analysis pipelines and visual exploration of datasets. It is distributed
296 under an open open-source³⁴ license (GNU General Public License, version 3). iSBatch handles the
297 data in a hierarchical fashion based on a source folder containing all data and little guidance
298 provided by the user. Due to memory limitations when handling large datasets, iSBatch alleviates
299 memory overload by loading only the minimum set of images required for a process. Garbage
300 collection is done after each cycle so effective memory limitations are imposed by the amount of
301 memory available in the system and not by the size of the database.

302 The software is designed for rapid exploration of large datasets and it includes an internal SQLite
303 database (<http://sqljet.com/>) for convenience. All files related to the iSBatch platform, including
304 source codes and API for developers can be accessed directly from the plugin website
305 (<https://github.com/SingleMolecule/iSBatch>).

306

307 **General workflow**

308

309 In the following subsections, we describe the general workflow and how to use the plugin for
310 accessing basic cellular information. iSBatch guides the user in the initial configuration steps to
311 proper categorization of the input data.

312 **Processing and Exploring Data - Custom functions**

313

314 iSBatch couples its hierarchical data structure management to an extended version of ImageJ's
315 macro interpreter. The user can record the executed operations, e.g. using ImageJ's built in macro
316 recorder, and simply copy and paste the code in iSBatch interpreter. After selecting the desired
317 parameters, the results are displayed, allowing the user to quickly check the results.

318 **Built-in functions**

319

320 Data preprocessing involves image operations as well. Image Flattening is available and follows the
321 equation

$$FlatImage = \frac{RawImage - BackgroundImage - CameraDarkCount}{BackgroundImage - CameraDarkCount} * ImageRange$$

322 where ImageRange depends on the image type (8-, 16- or 32-bit), the CameraDarkCount can be
323 provided either as a constant or an image; BackgroundImage, if not available, can be generated from
324 all images acquired. Generating the Background image may lead to biased correction if saturated
325 peaks or high intensity regions are found for long time in the movies. A Gaussian filter with a default
326 value of four pixels is applied to reduce the influence of bright spots.

327 Ideally, the background should be an image taken in the same conditions of the experiment prior to
328 have the sample in the Field Of View.

329 To allow for fast and accurate detection of peaks, we implemented the fluoroBancroft algorithm³⁵.
330 This algorithm localizes peaks with sub-diffraction limit accuracy without the need of numerical
331 fitting³⁶. All the results will be available in human-readable format like comma-separated-values
332 (csv).

333 Acquiring peak tables from the images configures a starting point of a whole new section of analysis
334 of single molecule data. Change point analysis is used to assign steps to single-molecule traces and
335 infer stoichiometry of molecules. Cellular ROIS can be either added manually or imported from
336 MicrobeTracker. In the later, a detailed subdivision of each cell with meshes is available. Therefore,
337 is possible to localize every peak in relation to the mesh and assign relative positions. With the
338 cellular parameters, such as cell length, width, area, can be obtained from the imported ROIs and an
339 artificial cell is created for the peaks to be inserted.

340 **Image Acquisition**

341 **Cell Culture**

342 Derivatives of *E. coli* K12 MG1655 carrying a chromosomal C-terminal fusions³⁷ containing DnaX-YPet
343 and DnaQ-mKate2 were grown overnight in M9 Minimal medium supplemented with Glycerol 2%
344 and 10mM thiamine hydrochloride; Cell cultures were diluted to 1:100 and grown from 4 hours at
345 37°C at 1100 rpm prior to the start of the imaging experiment.

346 **Image Acquisition**

347 The images were taken on a home-built single-molecule fluorescence microscope consisting of a
348 fully-automated inverted microscope body (Olympus IX-81) with excitation light provided by 514 nm
349 and 568 nm Sapphire lasers (Coherent) and equipped with a 1.49 NA 100x objective and a 512 ×
350 512 pixel EM-CCD camera (C9100-13, Hamamatsu). For imaging we used flow cells derivatized with
351 3-aminopropyl triethoxy silane (APTES, Sigma) and kept the flow at 10 µl/min.

352 The datasets are described as follows: 1) Rapid acquisition of DnaX-YPet and DnaQ-mKate2 each
353 containing 10 Fields of View. A Field of View comprises a reference bright field image and a
354 fluorescence movie (500 frames each with 34ms interval between acquisitions under different laser
355 intensities); 2) Time Lapse acquisition of DnaX-YPet and DnaQ-mKate2 containing 10 fields of View
356 containing a bright field and two fluorescent images of 50 ms for each fluorescent protein. The cycle
357 time is 20 minutes and the experiment was carried out for 400 minutes. Datasets are available as
358 supplementary materials S1 and S2;

359 **Conclusion**

360 We present here a fully open-source and community-driven ImageJ plugin for single-molecule
361 analysis focused on hierarchical data obtained from live-cell single-molecule experiments. The plugin
362 facilitates data exploration and bookkeeping of datasets with large number of images in multiple
363 colour channels, including basic pipelines and support for custom macros. We present case studies
364 that illustrate the ability to carry out analysis in a structured way, minimizing the burden of code
365 development. With this in mind, we envision that the user will be able to place a larger focus on

366 exploration of biological phenomena and new analysis routines. The development of open-source
367 analysis tools such as the ones presented here allows for a community-based sharing and
368 development³⁸ of the platforms required to analyse experiments that increasingly grow in complexity
369 and data richness. Software documentation is included within the Supplementary Material. The
370 source code is available for download at <https://github.com/SingleMolecule/iSBatch>.

371 Acknowledgements

372 We would like to thank M. Cox and E.A. Wood for providing the *E. coli* strain used in this work. The
373 authors would like to acknowledge funding from the Netherlands Organization for Scientific
374 Research (NWO; Vici 680-47-607) and the European Research Council (ERC Starting 281098). The
375 authors alone are responsible for the content and writing of the paper.

376 Conflict of interest

377 The authors declare that they have no conflicts of interest concerning this article.

378 References

- 379 1. Xia, T., Li, N. & Fang, X. Single-molecule fluorescence imaging in living cells. *Annu. Rev. Phys.*
380 *Chem.* **64**, 459–80 (2013).
- 381 2. Rigler, R. Fluorescence and single molecule analysis in cell biology. *Biochem. Biophys. Res.*
382 *Commun.* **396**, 170–175 (2010).
- 383 3. Reyes-Lamothe, R., Sherratt, D. J. & Leake, M. C. Stoichiometry and architecture of active
384 DNA replication machinery in *Escherichia coli*. *Science* **328**, 498–501 (2010).
- 385 4. Mashanov, G. I. Single molecule dynamics in a virtual cell: a three-dimensional model that
386 produces simulated fluorescence video-imaging data. *J. R. Soc. Interface* **11**, (2014).
- 387 5. Yu, J., Xiao, J., Ren, X., Lao, K. & Xie, X. S. Probing gene expression in live cells, one protein
388 molecule at a time. *Science* **311**, 1600–1603 (2006).
- 389 6. Haas, B. L., Matson, J. S., DiRita, V. J. & Biteen, J. S. Imaging Live Cells at the Nanometer-Scale
390 with Single-Molecule Microscopy: Obstacles and Achievements in Experiment Optimization
391 for Microbiology. *Molecules* **19**, 12116–12149 (2014).
- 392 7. Lenn, T. & Leake, M. C. Experimental approaches for addressing fundamental biological
393 questions in living, functioning cells with single molecule precision. *Open Biol.* **2**, 120090
394 (2012).

- 395 8. Cardona, A. & Tomancak, P. Current challenges in open-source bioimage informatics. *Nat. Methods* **9**, 661–5 (2012).
396
- 397 9. Eliceiri, K. W. *et al.* Biological imaging software tools. *Nat. Methods* **9**, 697–710 (2012).
- 398 10. Kametsky, L. *et al.* Improved structure, function and compatibility for cellprofiler: Modular high-throughput image analysis software. *Bioinformatics* **27**, 1179–1180 (2011).
399
- 400 11. Jones, T. R. *et al.* CellProfiler Analyst: data exploration and analysis software for complex image-based screens. *BMC Bioinformatics* **9**, 482 (2008).
401
- 402 12. Sliusarenko, O., Heinritz, J., Emonet, T. & Jacobs-Wagner, C. High-throughput, subpixel precision analysis of bacterial morphogenesis and intracellular spatio-temporal dynamics. *Mol. Microbiol.* **80**, 612–27 (2011).
403
404
- 405 13. Shivanandan, A., Radenovic, A. & Sbalzarini, I. F. MosaicIA: an ImageJ/Fiji plugin for spatial pattern and interaction analysis. *BMC Bioinformatics* **14**, 349 (2013).
406
- 407 14. Herbert, A. D., Carr, A. M. & Hoffmann, E. FindFoci: A Focus Detection Algorithm with Automated Parameter Training That Closely Matches Human Assignments, Reduces Human Inconsistencies and Increases Speed of Analysis. *PLoS One* **9**, e114749 (2014).
408
409
- 410 15. Abramoff, M. D., Magalhães, P. J. & Ram, S. J. Image processing with ImageJ Part II. *Biophotonics Int.* **11**, 36–43 (2005).
411
- 412 16. Schneider, C. a, Rasband, W. S. & Eliceiri, K. W. NIH Image to ImageJ: 25 years of image analysis. *Nat. Methods* **9**, 671–675 (2012).
413
- 414 17. Wollman, R. & Stuurman, N. High throughput microscopy: from raw images to discoveries. *J. Cell Sci.* **120**, 3715–22 (2007).
415
- 416 18. Sliusarenko. Microbetracker software. *Mol. Microbiol.* **80**, 612–627 (2012).
- 417 19. Stratmann, S. a & van Oijen, a M. DNA replication at the single-molecule level. *Chem. Soc. Rev.* **43**, 1201–20 (2014).
418
- 419 20. Robinson, A. & van Oijen, A. M. Bacterial replication, transcription and translation: mechanistic insights from single-molecule biochemical studies. *Nat. Rev. Microbiol.* **11**, 303–15 (2013).
420
421
- 422 21. Betzig, E. *et al.* Imaging intracellular fluorescent proteins at nanometer resolution. *Science* **313**, 1642–5 (2006).
423
- 424 22. Henriques, R., Griffiths, C., Hesper Rego, E. & Mhlanga, M. M. PALM and STORM: unlocking live-cell super-resolution. *Biopolymers* **95**, 322–31 (2011).
425
- 426 23. Zhu, L., Zhang, W., Elnatan, D. & Huang, B. Faster STORM using compressed sensing. *Nat. Methods* **9**, 721–3 (2012).
427
- 428 24. Team R Core Development. R: a language and environment for statistical computing | GBIF.ORG. *R Foundation for Statistical Computing* (2013). at <<http://www.r-project.org/>>
429

- 430 25. Thompson, R. E., Larson, D. R. & Webb, W. W. Precise nanometer localization analysis for
431 individual fluorescent probes. *Biophys. J.* **82**, 2775–83 (2002).
- 432 26. Hauberg, J. W. E. and D. B. and S. *GNU Octave version 3.0.1 manual: a high-level interactive*
433 *language for numerical computations.* (CreateSpace Independent Publishing Platform, 2009).
434 at <<http://www.gnu.org/software/octave/doc/interpreter>>
- 435 27. Leake, M. C. *et al.* Stoichiometry and turnover in single, functioning membrane protein
436 complexes. *Nature* **443**, 355–8 (2006).
- 437 28. Eckley, R. K. and I. A. changepoint: An R Package for Changepoint Analysis. *J. Stat.*
438 *Softw.* **58**, (2014).
- 439 29. Watkins, L. P. & Yang, H. Detection of intensity change points in time-resolved single-
440 molecule measurements. *J. Phys. Chem. B* **109**, 617–28 (2005).
- 441 30. Shcherbo, D. *et al.* Far-red fluorescent tags for protein imaging in living tissues. *Biochem. J.*
442 **418**, 567–574 (2009).
- 443 31. Shaner, N. C., Steinbach, P. A. & Tsien, R. Y. A guide to choosing fluorescent proteins. *Nat.*
444 *Methods* **2**, 905–909 (2005).
- 445 32. Muzzey, D. & van Oudenaarden, A. Quantitative time-lapse fluorescence microscopy in single
446 cells. *Annu. Rev. Cell Dev. Biol.* **25**, 301–27 (2009).
- 447 33. Schindelin, J. *et al.* Fiji: an open-source platform for biological-image analysis. *Nat. Methods*
448 **9**, 676–82 (2012).
- 449 34. Prlić, A. & Procter, J. B. Ten Simple Rules for the Open Development of Scientific Software.
450 *PLoS Comput. Biol.* **8**, 8–10 (2012).
- 451 35. Hedde, P. N., Fuchs, J., Oswald, F., Wiedenmann, J. & Nienhaus, G. U. Online image analysis
452 software for photoactivation localization microscopy. *Nat. Methods* **6**, 689–690 (2009).
- 453 36. Andersson, S. B. Localization of a fluorescent source without numerical fitting. *Opt. Express*
454 **16**, 18714–18724 (2008).
- 455 37. Datsenko, K. A. & Wanner, B. L. One-step inactivation of chromosomal genes in *Escherichia*
456 *coli* K-12 using PCR products. *Proc. Natl. Acad. Sci. U. S. A.* **97**, 6640–5 (2000).
- 457 38. Carpenter, A. E., Kametsky, L. & Eliceiri, K. W. A call for bioimaging software usability.
458 *Nature Methods* **9**, 666–670 (2012).

459

460 **Figure Captions**

461 **Figure 1 Schematic design of a single-cell, single-molecule experiment.** Panel A – Structure of a
462 time-lapse experiment. Each time point shows a bright-field (BF) image and its corresponding

463 fluorescence channel (in this example 568-nm excitation). The intervals are on the time scale of
464 minutes. Panel B – Monitoring of cell fluorescence intensity and its relation to total observable
465 protein concentration and protein number per cell throughout the experiment. Panel C – Structure
466 of a rapid-acquisition experiment. A single bright-field image is taken prior to subsequent rapid
467 image acquisition in the fluorescence channel (in this case 568-nm excitation). Panel D – Simulated
468 data of binding dynamics of a molecule.

469 **Figure 2 iSBatch Structure.** Panel A – Schematic representation of data structure (Experiment – E,
470 Sample – S, Field of View – FoV) and its connections. Panel B – Logic structure of the algorithm;
471 Panel C – User interface including ImageJ main panel (upper part) and iSBatch interface with the
472 main commands.

473 **Figure 3 Custom Macro runner.** iSBatch contains a custom macro runner that support syntax-
474 highlighting for creating, running and editing existing ImageJ macros and plugin commands from the
475 MacroRecorder.

476 **Figure 4 Built-in Peak Fitting Operation.** Panel A – Selected node highlighting the ‘Experiment’ level.
477 Panel B – Distribution of detected peak intensities within different ‘Samples’ in the same selected
478 ‘Experiment’ node for DnaQ-mKate2.

479 **Figure 5 Step-wise photobleaching.** Panel A – Selected node highlighting a ‘Field of View’ level.
480 Panel B – Selected cell within a ‘Field of View’ with the boundaries assigned in yellow and a selection
481 box in red. Panel C – Representative photobleaching trace of a detected focus. Red traces represent
482 the detected steps by change-point analysis algorithm.

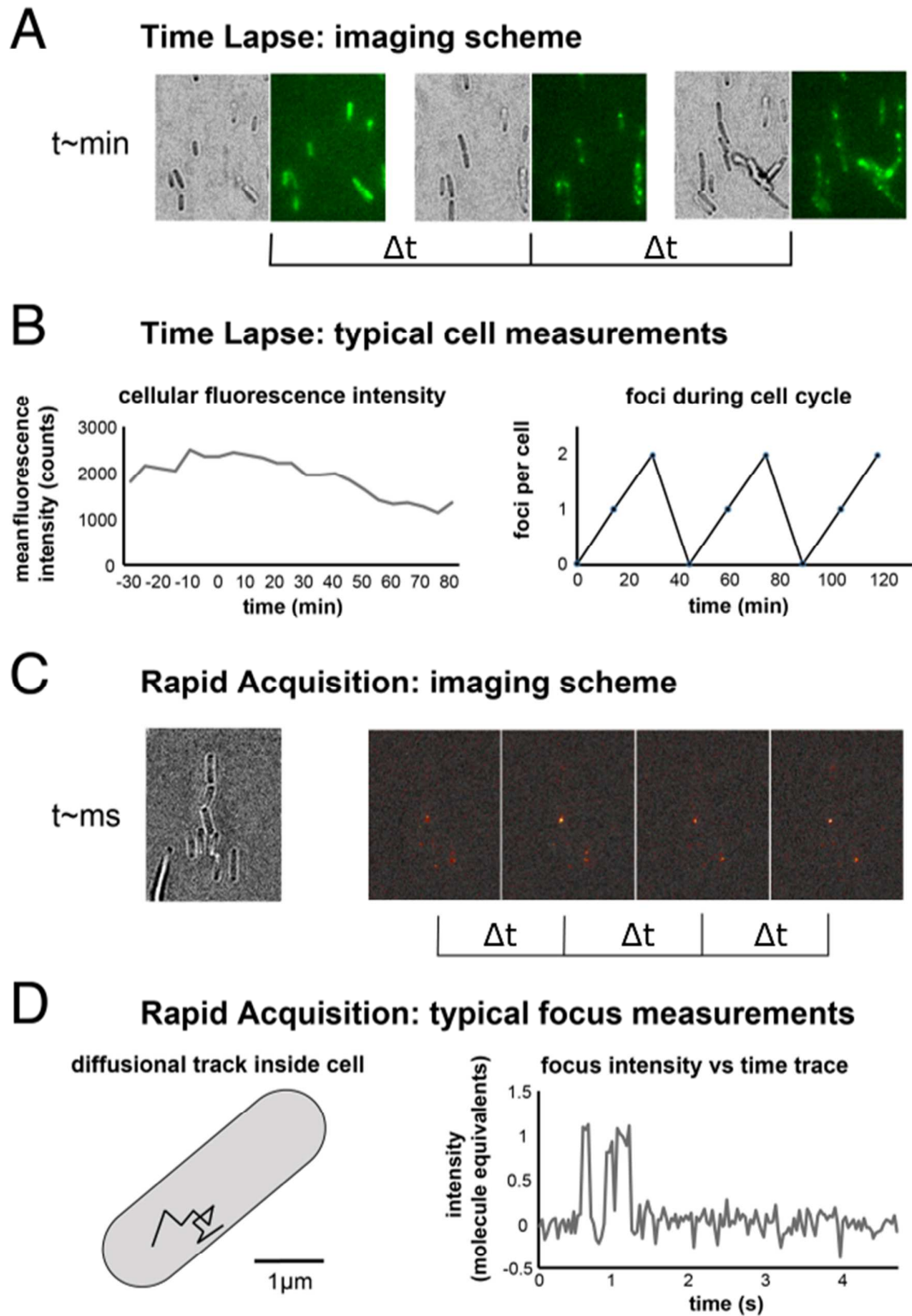
483 **Figure 6 Cellular fluorescence obtained by Rapid Acquisition.** Panel A – Selected node highlighting a
484 ‘Experiment’ level Panel B – Cellular fluorescence photobleaching dependent on laser intensity for
485 DnaQ-mKate2. Panel C – Selected node highlighting two ‘Samples’ selected within different
486 experiments. Panel D – Comparison of photobleaching properties of YPet and mKate2 when excited
487 with same laser intensity (180 W/cm^2).

488 **Figure 7 Particle tracking within cells.** Panel A – DnaQ-mKate2t particles tracked inside a live E. coli
489 cell. Blue: Confined track indicating protein bound to DNA. Panel B – Analysis of all detected focus
490 tracks within a ‘Sample’ level, e.g. DnaQ-mKate2 acquired at 180 W/cm^2 . Left panel shows the peak
491 lifetime distribution and right panel the calculated diffusion coefficient for the same population.

492 **Figure 8 Built-in Time-Lapse analysis.** Panel A – Fluorescence cell intensity over time for DnaX-YPet
493 and DnaQ-mKate2. Panel B – Number of long-lived immobile peaks per cell, i.e. foci. Panel C – Data
494 synchronization considering cell division times. Time zero is the first frame after cell division; cell
495 division time is 100 – 120 min. Panel D – Location maps. A projection of detected peaks in an
496 artificial, normalized cell. Left: projected cells with one detected focus, distributed towards the
497 *centre* of the cell; Right: projected cells with two detected foci, distributed towards the $\frac{1}{4}$ and $\frac{3}{4}$ of
498 the cell.

499

Figure 1.



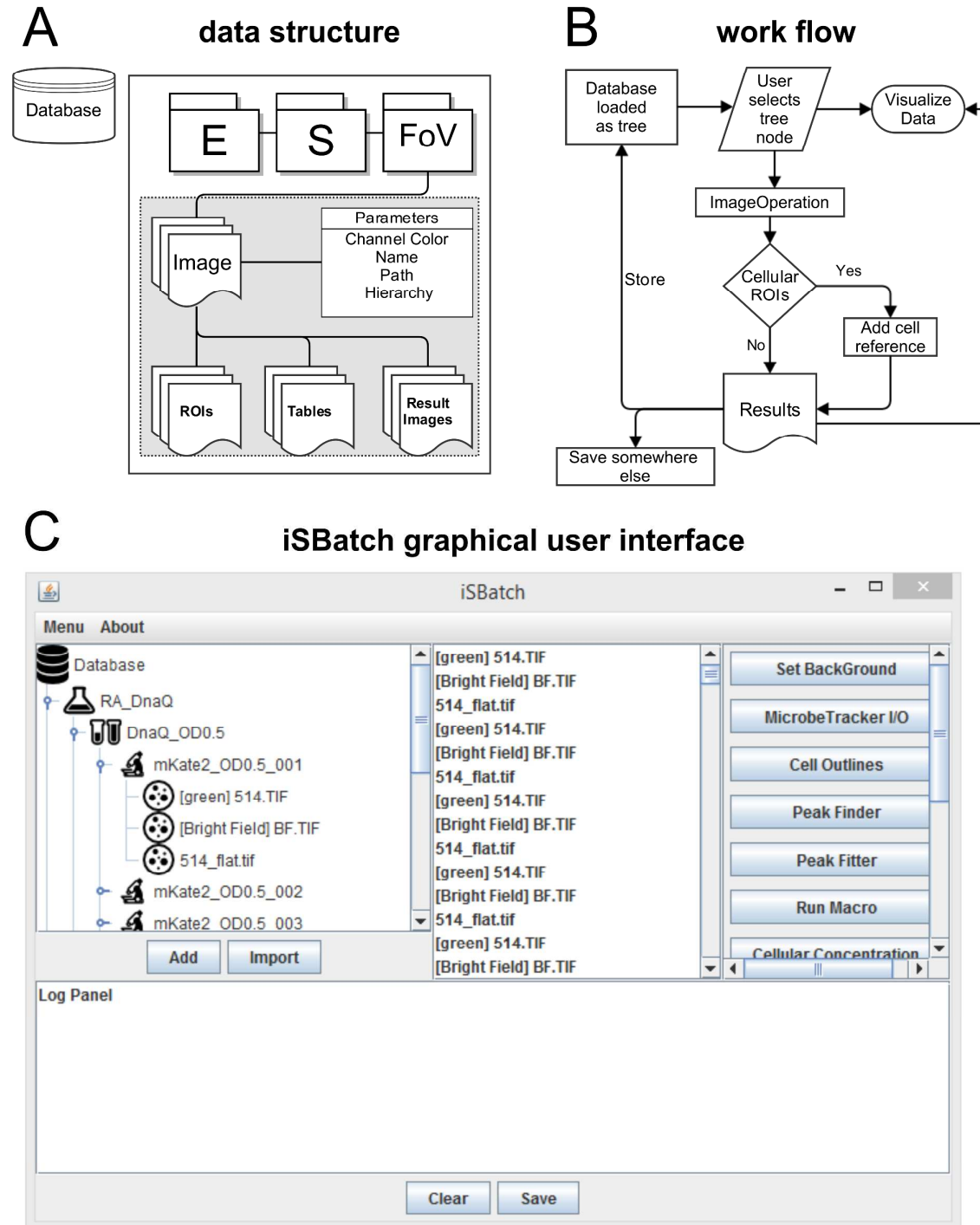
500

501

502

503 | Figure [34](#) Schematic design of a single-cell, single-molecule experiment. Panel A – Structure of a
504 time-lapse experiment. Each time point shows a bright-field (BF) image and its corresponding
505 fluorescence channel (in this example 568-nm excitation). The intervals are on the time scale of
506 minutes. Panel B – Exemplified cell fluorescence intensity and its relation to total observable protein
507 concentration and protein number per cell throughout the experiment. Panel C – Structure of a
508 rapid-acquisition experiment. A single bright-field image is taken prior to subsequent rapid image
509 acquisition in the fluorescence channel (in this case 568-nm excitation). Panel D – Simulated data of
510 binding dynamics of a molecule.

Figure 2.

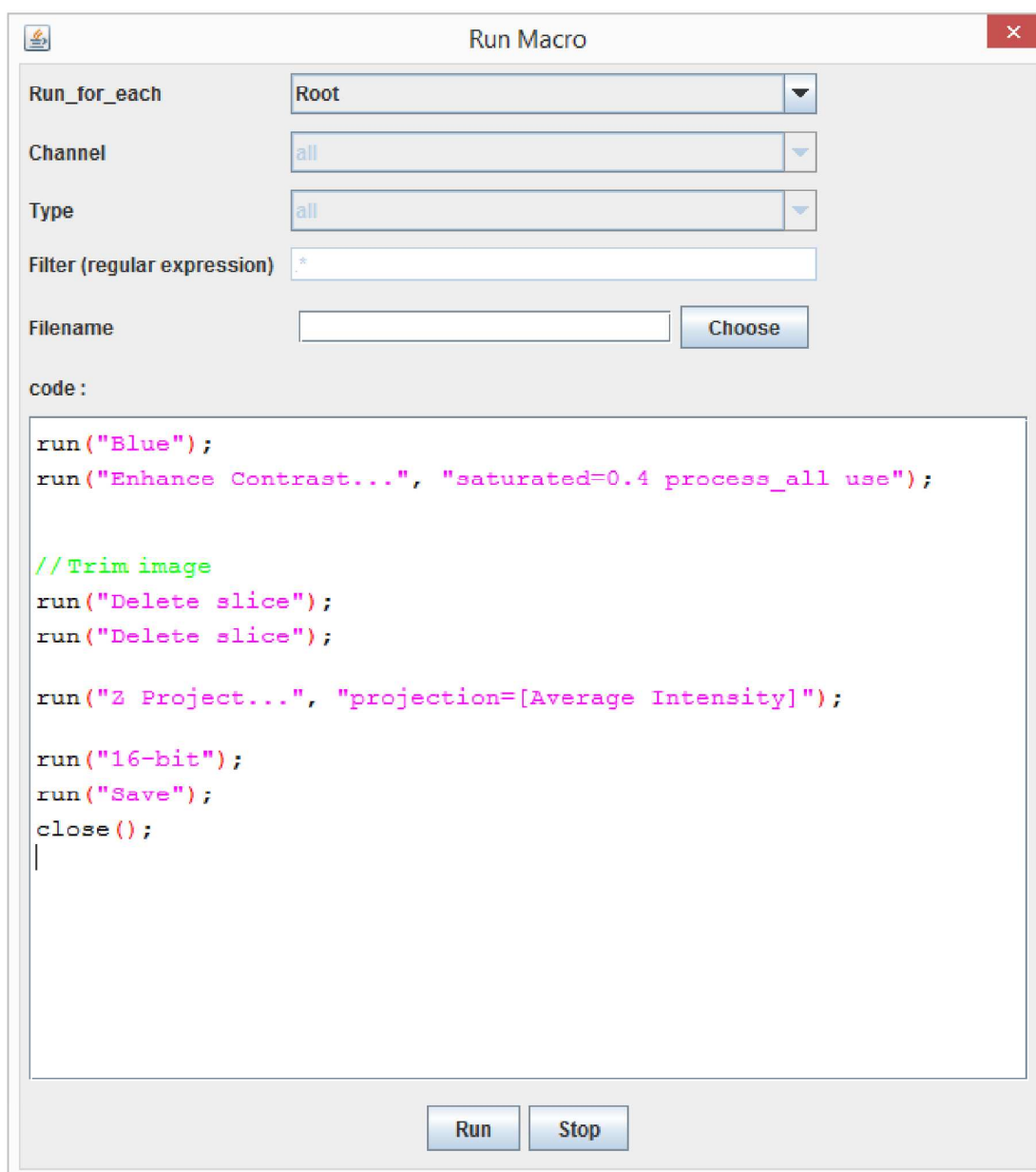


511

512 | Figure 42 iSBatch Structure. Panel A – Schematic representation of data structure (Experiment – E,
 513 Sample – S, Field of View – FoV) and its connections. Panel B – Logic structure of the algorithm;
 514 Panel C – User interface including ImageJ main panel (upper part) and iSBatch interface with the
 515 main commands.

Figure 3.

iSBatch *custom macro* panel



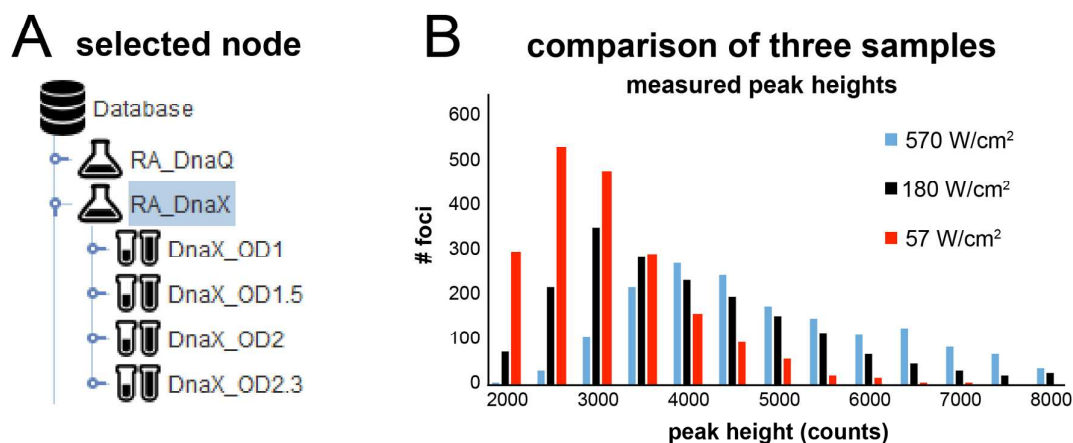
516

517 Figure 3 Custom Macro runner. iSBatch contains a custom macro runner that support syntax-
518 highlighting for creating, running and editing existing ImageJ macros and plugin commands from the
519 MacroRecorder.

520

521

Figure 4.



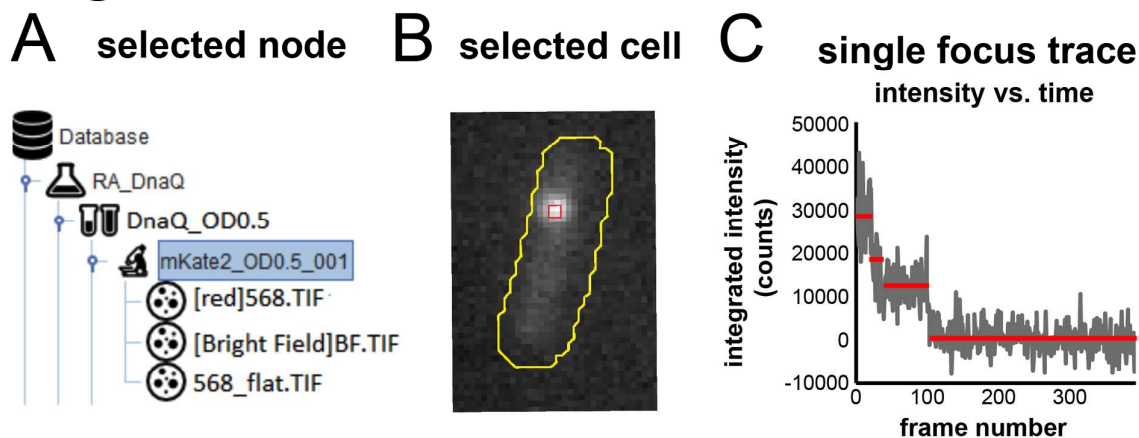
522

523 Figure 4 Built-in Peak Fitting Operation. Panel A – Selected node highlighting the ‘Experiment’ level.

524 Panel B – Distribution of detected peak intensities within different ‘Samples’ in the same selected

525 ‘Experiment’ node for DnaQ-mKate2.

Figure 5.



526

527

528 Figure 5 Step-wise photobleaching. Panel A – Selected node highlighting a ‘Field of View’ level. Panel

529 B – Selected cell within a ‘Field of View’ with the boundaries assigned in yellow and a selection box

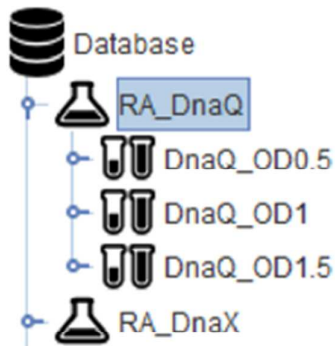
530 in red. Panel C – Representative photobleaching trace of a detected focus. Red traces represent the

531 detected steps by change-point analysis algorithm.

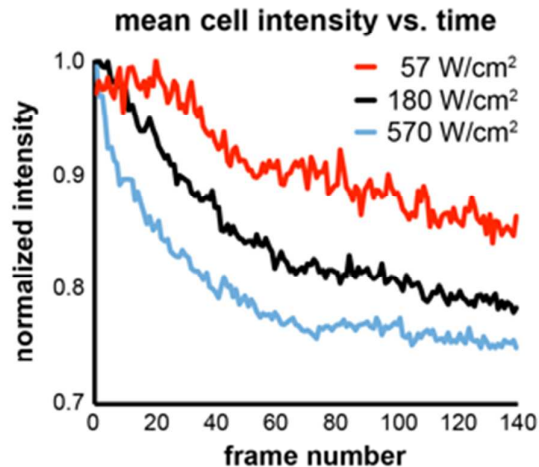
532

Figure 6.

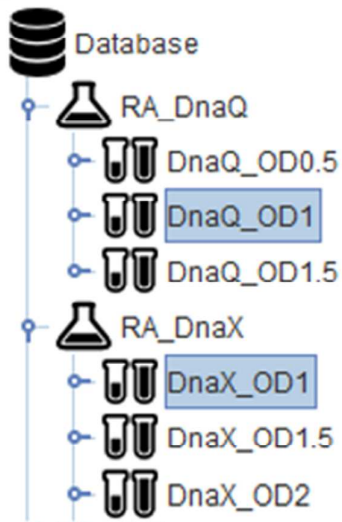
A selected node



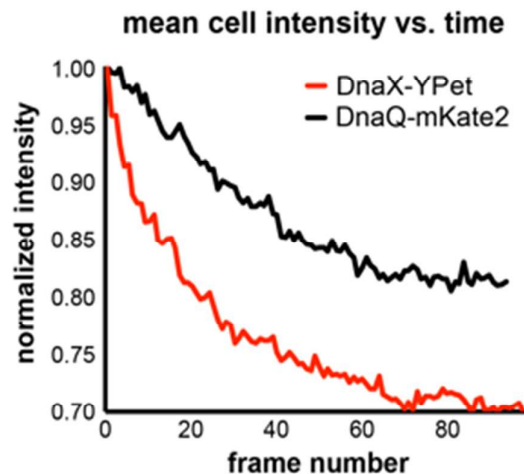
B comparison of three samples



C selected nodes



D comparison of two experiments:

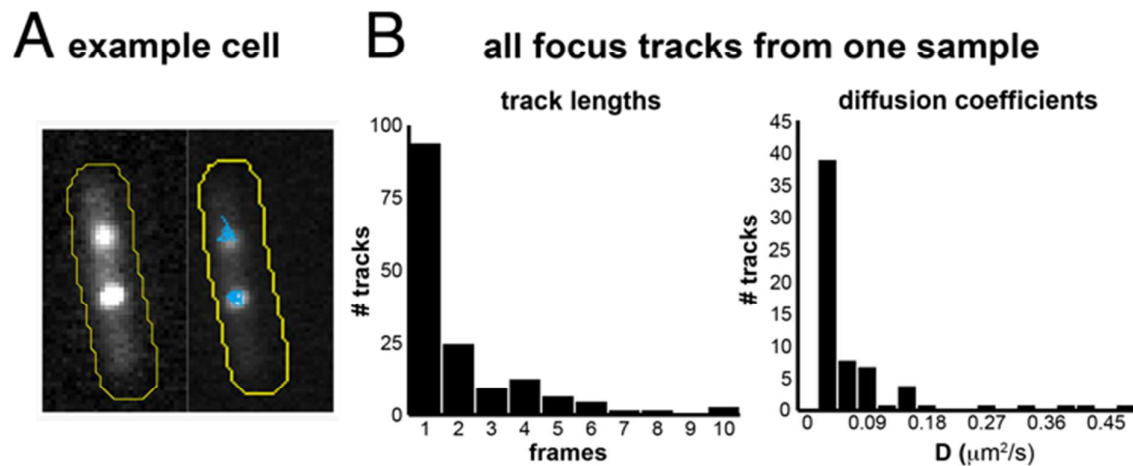


533

534

535 Figure 6 Cellular fluorescence obtained by Rapid Acquisition. Panel A – Selected node highlighting a
 536 ‘Experiment’ level Panel B – Dependence of cellular fluorescence photobleaching on laser intensity
 537 for DnaQ-mKate2. Panel C – Selected node highlighting two ‘Samples’ selected within different
 538 experiments. Panel D – Comparison of photobleaching properties of YPet and mKate2 when excited
 539 with same laser intensity (180 W/cm²).

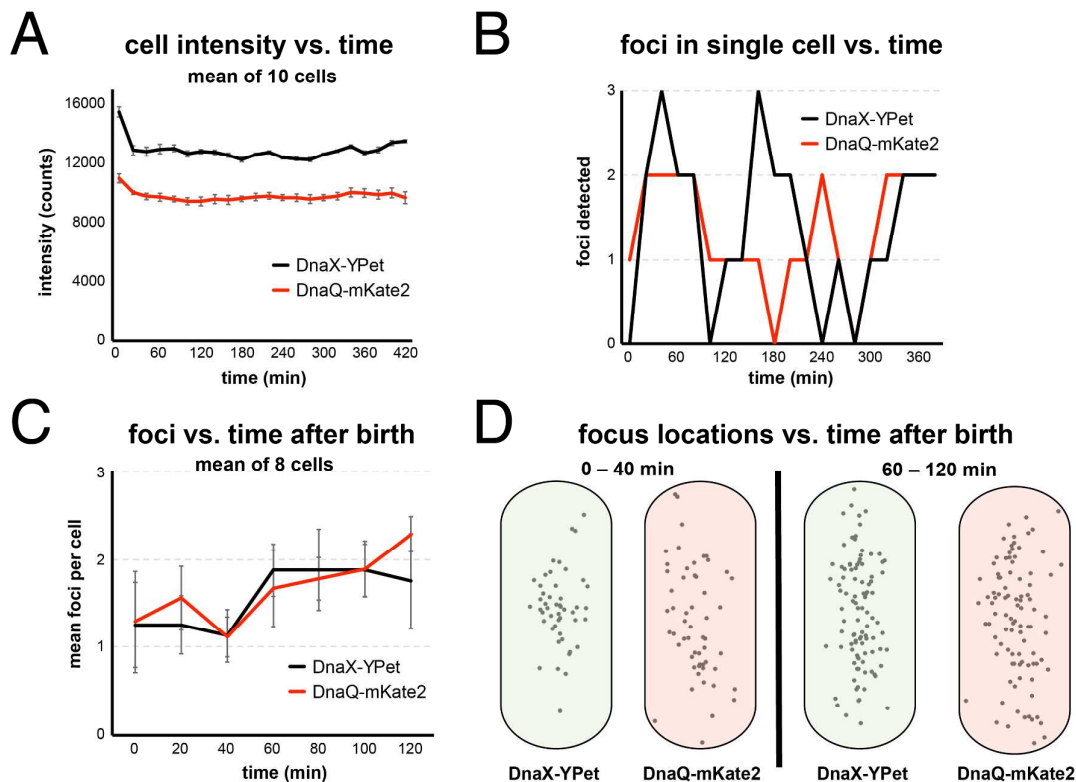
Figure 7.



540

541 Figure 7 Particle tracking within cells. Panel A – DnaQ-mKate2 particles tracked inside a live *E. coli*
 542 cell (fluorescence on the left, tracked positions on the right). The confined nature of the track
 543 indicates protein bound to DNA. Panel B – Analysis of all detected focus tracks within a ‘Sample’
 544 level, e.g. DnaQ-mKate2 acquired at 180 W/cm². Left panel shows the peak lifetime distribution and
 545 right panel the calculated diffusion coefficient for the same population.

Figure 8.



546

547 Figure 8 Built-in Time-Lapse analysis. Panel A – Fluorescence cell intensity over time for DnaX-YPet
548 and DnaQ-mKate2. Panel B – Number of long-lived immobile peaks per cell, i.e. foci. Panel C – Data
549 synchronization considering cell division times. Time zero is the first frame after cell division; cell
550 division time is 100 – 120 min. Panel D – Location maps. A projection of detected peaks in an
551 artificial, normalized cell. Left: projected cells with one detected focus, distributed towards the
552 centre of the cell; Right: projected cells with two detected foci, distributed more towards the $\frac{1}{4}$ and
553 $\frac{3}{4}$ positions in the cell.

554